
MobTCast: Leveraging Auxiliary Trajectory Forecasting for Human Mobility Prediction

Hao Xue

School of Computing Technologies
RMIT University
Melbourne, Australia
hao.xue@rmit.edu.au

Flora D. Salim

School of Computing Technologies
RMIT University
Melbourne, Australia
flora.salim@rmit.edu.au

Yongli Ren

School of Computing Technologies
RMIT University
Melbourne, Australia
yongli.ren@rmit.edu.au

Nuria Oliver

ELLIS Unit Alicante Foundation
Alicante, Spain
nuria@alum.mit.edu

Abstract

Human mobility prediction is a core functionality in many location-based services and applications. However, due to the sparsity of mobility data, it is not an easy task to predict future POIs (place-of-interests) that are going to be visited. In this paper, we propose MobTCast, a Transformer-based context-aware network for mobility prediction. Specifically, we explore the influence of four types of context in the mobility prediction: temporal, semantic, social and geographical contexts. We first design a base mobility feature extractor using the Transformer architecture, which takes both the history POI sequence and the semantic information as input. It handles both the temporal and semantic contexts. Based on the base extractor and the social connections of a user, we employ a self-attention module to model the influence of the social context. Furthermore, unlike existing methods, we introduce a location prediction branch in MobTCast as an auxiliary task to model the geographical context and predict the next location. Intuitively, the geographical distance between the location of the predicted POI and the predicted location from the auxiliary branch should be as close as possible. To reflect this relation, we design a consistency loss to further improve the POI prediction performance. In our experimental results, MobTCast outperforms other state-of-the-art next POI prediction methods. Our approach illustrates the value of including different types of context in next POI prediction.

1 Introduction

Human mobility prediction plays an important role in a wide range of applications, including personalised advertisement, traffic modelling, crowd management and predicting the spread of pandemics [14, 17]. For example, targeted advertisements, such as store information and coupons can be delivered precisely by predicting the future POIs that users might visit. From a public policy perspective, traffic congestion may be reduced by leveraging traffic prediction to inform decisions relative to public space planning and traffic road network design.

Unlike other densely acquired trajectory sequence data (such as trajectories extracted from videos [1, 32, 20] and GPS trajectories [21, 31]), trajectory data for the next POI prediction task is typically in the form of check-in sequences and collected from popular Location Based Social Networks (LBSNs),

such as Foursquare. As the visited POI information is recorded only when a user chooses to check-in and accesses the location service, the check-in sequence data is very sparse. Due to privacy concerns or battery limitations on mobile devices, users rarely report their locations all the time. This inherent sparsity increases the difficulty of the prediction of future POIs dramatically.

In the last few years, given major advances in deep learning techniques and especially the success of applying Recurrent Neural Networks (RNNs) for sequence prediction tasks, many research works have leveraged the user’s historical trajectories to predict most likely POI to be visited by that user. A pioneering work proposed ST-RNNs [26] which employ both time-specific and distance-specific transition matrices in an RNN architecture to model time intervals and geographical distances between two consecutive check-in POIs in historical trajectories. DeepMove [9] incorporates a historical attention module to capture the periodicity of human mobility. Following this trend, more recently, VANext [11] and ACN [29] propose two more attention mechanisms to learn long term preferences for users from history trajectories. However, considering the data sparsity, only exploring the historical visiting information may not be enough. For instance, compared to the large number of POIs and the complexity of the nature of people’s preferences, the small amount of visited POIs in a user’s historical log is unlikely to reveal their entire range of preferences over all available POIs. Therefore, in addition to exploring the *temporal context* based on the user’s own past visiting history, the influence from other types of context could be valuable to achieve more accurate POI prediction. In particular, there are three important types of context that could help tackle the sparsity problem: (1) *Semantic Context*: Typically, in LBSNs, each POI belongs to a category with high level semantic meanings such as *Shops* and *Education*. This context is an indicator in predicting the next POI. For example, people are more likely to visit *Food* POIs at lunch time than at other times. Leisure travellers will tend to check-in at tourism POI attractions. (2) *Social Context*: Friends and family members often visit a POI together. A user may also check-in a new POI recommended by friends. (3) *Geographical Context*: POIs that are close to each other might be visited by the same user due to their proximity. For example, a user may visit a shopping mall and then go to a nearby cinema. A detailed data-driven analysis of these contexts is given in Section 7.2.

However, one limitation in the existing literature is that the context has been typically modelled based on manually designed functions. For example, Sun *et al.* [33] noticed that the geographical distances between any two non-consecutive visited POIs are also important. A geo-nonlocal function is introduced into the RNN to measure the distance between each visited POI and the average location of all visited POIs. Similarly, Flashback [41] introduces a manually designed weighting function to assign weights based on both temporal and geographical distances for each time step.

In this paper, we propose a novel method called MobTCast, for the next POI prediction task, which is explicitly designed to model and incorporate the influence of the aforementioned contexts in a data-driven manner. A Transformer [35]-based mobility feature extractor is a fundamental component in MobTCast to perform the main POI prediction task. It takes both the visited POI history and the semantic category information to learn semantic-aware mobility features. Using this mobility feature extractor, we extract not only the semantic-aware mobility features of a user but also the features of his/her neighbours. A self-attention mechanism is then applied to model the social influence from neighbours to the user. This aggregated feature is both semantic and social-aware. To include geographical context, the model includes an auxiliary task, which is different from previously proposed methods that depend on manually designed kernels. Considering that the focus of this auxiliary task is exploring the geographical information (i.e., geographical coordinates of visited POIs), it is designed as a trajectory forecasting task. The purpose is predicting a future location based on the previously visited locations.

As a result of these two tasks (main and auxiliary), there are two predicted coordinates available: the predicted location from the auxiliary trajectory forecasting task and the inferred location from the predicted POI given by the main task. Ideally, the Euclidean distance between these two locations should be as close as possible. To this end, a novel consistency loss function is proposed to reflect and embody this relationship in the training process of MobTCast. Thus, the main and the auxiliary tasks are connected not only at the feature level but also at the output level. We conduct extensive experiments on three publicly available real-world datasets. The results demonstrate MobTCast’s competitive POI prediction performance and show the value of incorporating different types of context as well as the consistency loss function.

In summary, the main contributions of our work are two-fold: (i) We address the next POI prediction problem by including four types of context: temporal, geographical, social and semantic. Moreover, we design an auxiliary trajectory forecasting task to predict the geographical coordinates of the next most likely location. To the best of our knowledge, this is the first time that auxiliary trajectory forecasting is incorporated in a POI prediction model, which provides a new perspective for understanding human mobility. (ii) We introduce a novel consistency loss function to connect the predicted POI (from the main task) and the predicted location (from the auxiliary task). This consistency loss function helps further improve the POI prediction performance.

2 Related Work

Next POI Prediction One of the earliest works that utilised geographical, temporal, and social contexts to predict the next POI is [6], which combines the periodic day-to-day mobility patterns with information from social ties, inferred from the friendship network. Since this seminal work, many others have proposed methods to better model the check-in behaviours or the trajectory of geographical movements, depending on the data they work on. Based on weight matrix factorisation, Cheng *et al.* [4] proposed a personalised Multi-centre Gaussian Model (MGM) to capture the geographical influence and Lian *et al.* [23] proposed GeoMF model that considers the geographical influence. Li *et al.* [22] developed a ranking based geographical factorisation method to incorporate the influences of geographical and temporal context. Recently, a local geographical model is introduced into the logistic matrix factorisation to improve the accuracy of POI recommendation [30]. GERec [36] employs a spatio-temporal relation path embedding to model the temporal, spatial and semantic content for next POI recommendation.

Deep learning-based neural networks have been used for temporal sequence modelling. RNNs (including LSTM [15] and GRU [7]) and Transformer [35] have also been proposed and successfully applied to many time series prediction problems such as pedestrian trajectory prediction [1, 39] and traffic prediction [38]. For the next POI prediction task, ST-RNN (Spatial Temporal Recurrent Neural Networks), proposed by Liu *et al.* [26], improves the original RNN architecture by incorporating temporal and spatial context at each time interval in the historical trajectory. Following the trend of using RNN, a series of methods are proposed to model human mobility behaviours and predict the next POI, such as DeepMove [9]. Based on RNNs, it applies an attention mechanism to capture the periodical features of human mobility. Similarly, Gao *et al.* [11] introduced a variational attention mechanism to learn the attention on the historical trajectories.

Efforts have also been made to incorporate different kinds of context for POI prediction. SERM [43] is designed to jointly learn embeddings of temporal and semantic contexts (i.e., text messages). Gao *et al.* [13] proposed to leverage a knowledge graph to accommodate the influence of users, locations and semantics. Flashback [41] tackles the geographical context through an explicitly designed spatio-temporal weighting function. The calculated weights are applied to the hidden states in an RNN correspondingly. STAN [28] incorporates the geographical context to learn the regularities between non-adjacent locations and non-contiguous visits. In these methods, the modelling of the geographical context heavily depends on manually designed kernel functions (e.g., Euclidean distance based functions) or a pre-computed spatio-temporal relation matrix [28] (which would dramatically increase the memory and computation costs when the total number of POIs is large). There is limited work on that have simultaneously considered temporal, semantic, social and geographical contexts.

Auxiliary Task Learning An auxiliary task is a task that is trained jointly with the main task during the training phase to enhance the main task’s performance. As a variant of multi-task learning, auxiliary learning have become popular in recent years. In computer vision, it has been used for semantic segmentation [25, 5], crowd counting [45], depth completion [27], and localisation [34].

Recently, several methods have been proposed using multi-task learning to model human mobility. For example, Chen *et al.* [3] introduced DeepJMT which jointly predicts location and time. MCARNN, proposed by Liao *et al.* [24], is a multi-task network to predict both activity and location. Compared to multi-task learning, in auxiliary task learning the auxiliary task is nonoperational during the inference phase. Note that in MCARNN [24], the authors also proposed to leverage an auxiliary task to learn location embeddings. However, the auxiliary task in the proposed MobTCast approach is a trajectory forecasting task, which is designed to consider the geographical context directly, with the introduction of a consistency loss function to connect the main task and the auxiliary task.

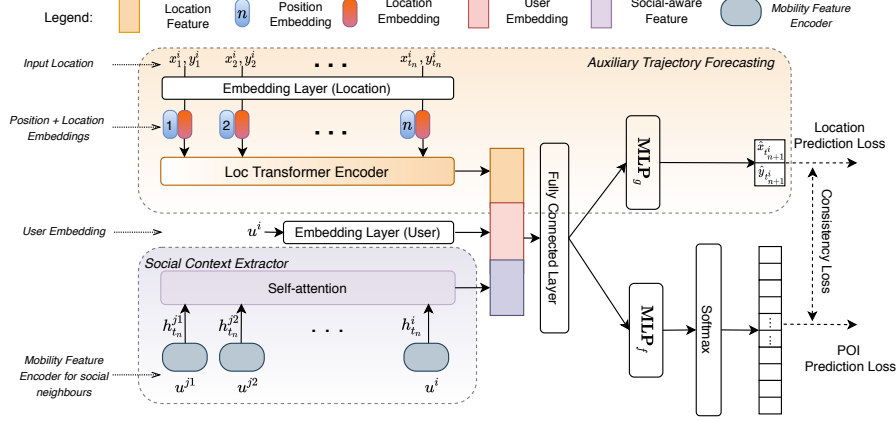


Figure 1: The proposed MobTCast. Dash arrows indicate operations used in the training phase only. Due to space limitations, please refer to Figure 2(a) for details of the Mobility Feature Encoder.

3 Problem Formulation

Consider two sets: $\mathbf{P} = \{poi_1, poi_2, \dots, poi_{|P|}\}$ and $\mathbf{U} = \{u^1, u^2, \dots, u^{|\mathbf{U}|}\}$, denoting the set of POIs and the set of users, respectively. Each POI is represented by a (lon, lat) tuple, which indicates the geographical context. The human mobility prediction problem is defined as follows. Given the history mobility trajectory $T^i = (p_{t_1}^i, p_{t_2}^i, \dots, p_{t_n}^i)$ of user $u^i \in \mathbf{U}$, the goal is to predict the POI $\hat{p}_{t_{n+1}}^i$ that is going to be visited by the same user at the next time t_{n+1}^i . Here, $p_{t_n}^i \in \mathbf{P}$ stands for the POI visited by user u^i at time t_n and the geographical coordinate of $p_{t_n}^i$ is indicated by $(x_{t_n}^i, y_{t_n}^i)$. The observation length of the given history trajectory is n .

Based on the geographical coordinates, the semantic category information $c_{t_n}^i$ can be acquired. Note that depending on the dataset, we utilise two types of POI category hierarchies given by: ArcGIS¹ and Foursquare². The social context of user u^i , is given by his/her neighbours, represented as $\mathcal{N}_{(i)} = \{u^{j1}, u^{j2}, \dots, u^{jm}\}$, which is a group of users (in \mathbf{U}) socially connected with user u^i .

4 Method

The overall framework of the proposed method is illustrated in Figure 1. To solve the POI prediction task and the auxiliary trajectory forecasting task, MobTCast consists of four major components: (i) **Mobility Feature Extractor** (Section 4.1): this is a fundamental component in the proposed POI prediction method. It is used to extract semantic-aware mobility features of a given history trajectory. The temporal context is also modelled in this extractor. (ii) **Social Context Extractor** (the light purple part in Figure 1, Section 4.2): this module is used to model the social influence of user u^i in the prediction process. (iii) **Auxiliary Trajectory Forecasting** (the light orange part in Figure 1, Section 4.3): this auxiliary task is introduced to incorporate the geographical context in the POI prediction, to explicitly predict the next geo-location. (iv) **Consistency Loss**: (Section 4.4) this component establishes a relationship between the auxiliary trajectory forecasting and the POI prediction. It is designed to better leverage the auxiliary task and further improve the performance. The detailed description of each component is presented in the following subsections.

4.1 Semantic-aware Mobility Feature Extractor

The modelling of the given history trajectory of a user is an essential step in any POI prediction method. In MobTCast, this step is tackled as a mobility feature extraction process. In addition to the visited POIs and the visited timestamps that have been widely considered by other methods [9], we argue that the semantic context plays a significant role and should also be incorporated in this process. For example, *Alice* visited a *Sushi Shop* for lunch yesterday but she decides to go to *McDonald's*

¹<https://developers.arcgis.com/rest/geocode/api-reference/geocoding-category-filtering.htm>

²<https://developer.foursquare.com/docs/build-with-foursquare/categories/>

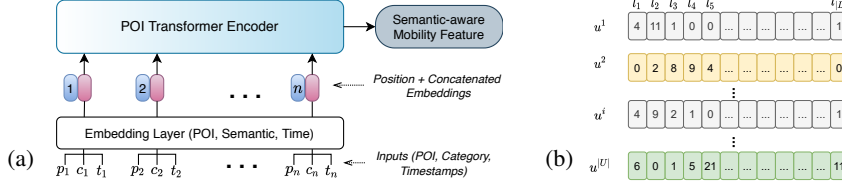


Figure 2: (a) Illustration of the proposed Transformer-based mobility feature extractor. (b) Illustration of using check-in vectors for discovering neighbours (u^1 is a neighbour of u^i).

today. Although *Sushi Shop* and *McDonald's* are two different POIs, they belong to the same semantic category *Food*. Such a high-level semantic context is helpful to predict which POI is going to be visited by *Alice* tomorrow noontime.

To incorporate the semantic context, a Semantic-aware Mobility Feature Extractor is explicitly designed. As shown in Figure 2(a), this feature extractor takes three types of inputs: POIs, timestamps, and semantic category labels. The mobility feature extraction process can be formulated as:

$$e_p^{i,t} = \phi_p(p_t^i; \mathbf{W}_{\phi_p}), e_c^{i,t} = \phi_c(c_t^i; \mathbf{W}_{\phi_c}), e_t^{i,t} = \phi_t(t_t^i; \mathbf{W}_{\phi_t}), \quad (1)$$

$$e^{i,t} = e_p^{i,t} \oplus e_c^{i,t} \oplus e_t^{i,t}, \quad (2)$$

$$h_{t_n}^i = \mathcal{F}(e^{i,t_1}, e^{i,t_2}, \dots, e^{i,t_n}; \mathbf{W}_{\mathcal{F}}), \quad (3)$$

where \oplus is the concatenation operation and $e^{i,t}$ is the concatenated embedding of: the POI embedding $e_p^{i,t}$, the semantic category embedding $e_c^{i,t}$, and the temporal embedding $e_t^{i,t}$. In these equations, the \mathbf{W} terms stand for the weight matrices that need to be optimised during the training process. These three embedding vectors are calculated through three different embedding layers ($\phi_p(\cdot)$, $\phi_c(\cdot)$, and $\phi_t(\cdot)$), respectively. In Eq. (3), $\mathcal{F}(\cdot)$ is a function to extract feature $h_{t_n}^i$ with embedding vectors of the whole history trajectory from t_1 to t_n as input. This extracted feature $h_{t_n}^i$ models the spatio-temporal history movement behaviour of user u^i and it is semantic-aware as well. In MobTCast, the Transformer architecture [35] is used as $\mathcal{F}(\cdot)$ as it has been proven effective in other sequence modelling tasks, such as language understanding [8], speech recognition [37], flow prediction [40], and video action recognition [12]. The Transformer architecture is based on a self-attention mechanism so it can better model the history trajectory movement than a vanilla RNN structure. Since there is no recurrence or convolution operation in the Transformer, position embeddings are added to the concatenated embeddings to retain sequential order information (see Figure 2(a)). We use standard sine/cosine function based position embeddings introduced in [35].

4.2 Social Context Extractor

The social influence is another important kind of context to be considered in the next POI prediction process, especially when the mobility data is sparse. For example, one of *Alice's* friends recommends a new restaurant that she has never visited before, so she decides to visit it tomorrow. In this example, since there is a high likelihood that this restaurant has been visited by *Alice's* friend before, the social context of (*Alice's* friend's mobility) is helpful to predict *Alice's* next POI.

Inferring social links based on mobility data is yet another challenging task [2, 10, 16]. Since our main focus is POI prediction, we adopt a straightforward approach to discover the neighbour set $\mathcal{N}_{(i)}$ of user u^i . The social neighbour discovering process is as follows. As shown in Figure 2(b), we first build a check-in vector for each user, based on their check-in history. The dimension of this check-in vector equals the number of POIs ($|P|$) and each dimension of the vector indicates how many times the user visited the corresponding POI. The cosine similarity of two users' check-in vectors is then computed. If the calculated cosine distance is larger than a threshold τ , these two users are considered to be connected.

For each user $u^j \in \mathcal{N}_{(i)}$, the mobility feature extractor (Eqs. (1) - (3)) is applied to calculate the semantic-aware mobility feature $h_{t_n}^j$. It worth noting that any "future" information (after t_n^i) from neighbours cannot be used as it is not available for the prediction time step t_{n+1}^i . If t_n^j is the last timestamp of a neighbour's observed trajectory, mathematically, the above condition can be represented as: $t_n^j \leq t_n^i, \forall j \in \mathcal{N}_{(i)}$. The extraction of social influence can be seen as a feature

aggregation process. The social context vector $H_{t_n}^i$ is a weighted sum of his/her own mobility feature $h_{t_n}^i$ and his/her neighbour’s (all neighbours in $\mathcal{N}(i)$ are considered) mobility feature $h_{t_n}^j$:

$$H_{t_n}^i = \alpha_i h_{t_n}^i + \sum_{j \in \mathcal{N}(i)} \alpha_j h_{t_n}^j \quad (4)$$

To compute the weight terms α , we use a multi-head self-attention mechanism [35].

4.3 Auxiliary Trajectory Forecasting

Compared to other recommendation tasks, like next shopping item prediction and music recommendation, the geographical proximity of POIs is an inherent characteristic in the next POI prediction task. For example, *Alice* is more likely to visit POIs (e.g., a *supermarket* to buy snacks or a *park* to walk) that are geographically close to the visited *Sushi Shop* than those that are significantly further away. This geographical information is thus another important type of context that is worthy to exploit in the next POI prediction task.

Unlike previously published efforts [23, 44, 13, 41] that take the geographical information into account by manually designed kernel functions, the geographical context is incorporated in MobTCast by leveraging an auxiliary task. This auxiliary task is designed as a trajectory forecasting task. Since POI prediction is typically tackled as a classification task, the long tail distribution of POIs caused by data sparsity is a severe bottleneck that limits the performance. Thus, the motivation of this introduced auxiliary trajectory forecasting is to directly forecast geo-location (as a location regression task) to leverage the geographical context and alleviate the effect of data sparsity.

Similar to the pedestrian trajectory prediction task [19, 39], the coordinates of the historical trajectory are firstly embedded through an embedding layer ϕ_l . Then, another Transformer \mathcal{F}_g is used to extract the geographical context vector $g_{t_n}^i$. Mathematically, this process is expressed as follows:

$$e_l^{i,t} = \phi_l(x_t^i, y_t^i; \mathbf{W}_{\phi_l}), \quad (5)$$

$$g_{t_n}^i = \mathcal{F}_g(e_l^{i,t_1}, e_l^{i,t_2}, \dots, e_l^{i,t_{n-1}}; \mathbf{W}_{\mathcal{F}_g}), \quad (6)$$

where \mathbf{W} terms are trainable weights. To build a connection between the main task and the auxiliary task, the social context vector $H_{t_n}^i$ from the social context extractor (Section 4.2) and the geographical context vector $g_{t_n}^i$ are concatenated and then passed through a fully connected layer ($\text{FC}(\cdot)$). In addition, the user embedding that learns the personalised user preference is also included as the user’s personal preference would also influence his/her own mobility pattern:

$$e_u^i = \phi_u(u^i; \mathbf{W}_{\phi_u}), \quad (7)$$

$$f_{t_n}^i = \text{FC}(h_{t_n}^i \oplus g_{t_n}^i \oplus e_u^i). \quad (8)$$

Since the user embedding e_u^i remains the same during the whole trajectory, it is only used in Eq. (8) and not used at every time step like other embeddings in Eq. (3) or Eq. (6).

This aggregated feature representation $f_{t_n}^i$ inherits the semantic context, the social context, the geographical context, and the user personal preference. It then can be used for both the main (i.e. predicting the next POI, detailed in the following subsection) and the auxiliary tasks. The predicted location $(\hat{x}_{t_{n+1}}^i, \hat{y}_{t_{n+1}}^i)$ at time step t_{n+1}^i is then decoded via:

$$(\hat{x}_{t_{n+1}}^i, \hat{y}_{t_{n+1}}^i) = \text{MLP}_g(f_{t_n}^i), \quad (9)$$

where $\text{MLP}_g(\cdot)$ is a multi-layer perceptrons (MLP)-based decoder.

4.4 Next POI Prediction

Based on the context-aware feature $f_{t_n}^i$, the prediction of POI at next time step t_{n+1}^i is as follows:

$$\Pr(\hat{p}_{t_{n+1}}^i) = \text{softmax}(\text{MLP}_f(f_{t_n}^i)), \quad (10)$$

where $\text{MLP}_f(\cdot)$ is another MLP structure. Different from the auxiliary trajectory forecasting (Eq. (9)), an extra softmax layer is required for generating the probabilities of all POIs. Thus, by performing

Eq. (10), the most likely POI that will be visited by the user u^i at the time step t_{n+1}^i is the one with the largest probability in $\Pr(\hat{p}_{t_{n+1}}^i)$.

In addition to the POI prediction loss \mathcal{L}_1 for the main task and the trajectory forecasting loss \mathcal{L}_2 for the auxiliary task, we propose a novel consistency loss \mathcal{L}_3 for training MobTCast. The details of these losses are described below.

POI Prediction Loss Given that the next POI prediction is treated as a classification over the entire POI set, the POI prediction loss is a multi-class cross entropy loss:

$$\mathcal{L}_1 = - \sum_{p=1}^{|P|} \Pr(p_{t_{n+1}}^i)_p \log(\Pr(\hat{p}_{t_{n+1}}^i)_p), \quad (11)$$

where $\Pr(p_{t_{n+1}}^i)_p$ indicates the ground truth, i.e., $\Pr(p_{t_{n+1}}^i)_p = 1$ if u^i visited the p -th POI at t_{n+1}^i . Similarly, $\Pr(\hat{p}_{t_{n+1}}^i)_p$ is the predicted probability that the user u^i will visit the p -th POI.

Trajectory Forecasting Loss This loss is used for the auxiliary task. It is a mean square error loss that measures the difference between the predicted location and the ground truth location.

$$\mathcal{L}_2 = \|\hat{x}_{t_{n+1}}^i - x_{t_{n+1}}^i\|^2 + \|\hat{y}_{t_{n+1}}^i - y_{t_{n+1}}^i\|^2, \quad (12)$$

where $(x_{t_{n+1}}^i, y_{t_{n+1}}^i)$ is the geographical coordinate of the ground truth POI $p_{t_{n+1}}^i$ that is visited by u^i at t_{n+1}^i .

Consistency Loss To better leverage the auxiliary task, we not only connect the main task and the auxiliary task at the feature level (Eq. (8)) but also design a new loss function to further link the two tasks. Intuitively, there should be a relationship between the predicted POI from the main task and the predicted location from the auxiliary task. That is, the location of the predicted POI and the predicted location should be as close as possible. Consequently, a consistency loss is introduced to embody the above relationship.

Based on the probabilities $\Pr(\hat{p}_{t_{n+1}}^i)$ given by Eq. (10), the location of the predicted POI can be inferred through:

$$\operatorname{argmax}(\Pr(\hat{p}_{t_{n+1}}^i)) \Rightarrow (\tilde{x}_{t_{n+1}}^i, \tilde{y}_{t_{n+1}}^i). \quad (13)$$

The consistency loss is then defined as the mean squared error between the inferred location $(\tilde{x}_{t_{n+1}}^i, \tilde{y}_{t_{n+1}}^i)$ and the predicted location $(\hat{x}_{t_{n+1}}^i, \hat{y}_{t_{n+1}}^i)$:

$$\mathcal{L}_3 = \|\tilde{x}_{t_{n+1}}^i - \hat{x}_{t_{n+1}}^i\|^2 + \|\tilde{y}_{t_{n+1}}^i - \hat{y}_{t_{n+1}}^i\|^2. \quad (14)$$

Note that, as given in Eq. (15), both \mathcal{L}_2 and \mathcal{L}_3 (mean squared errors) are calculated and average over all training samples in a batch.

The overall loss function is a combination of the above three losses so that the parameters of our MobTCast are optimised by minimising:

$$\mathcal{L} = \sum_{b=1}^B (\theta_1 \mathcal{L}_1^b + \theta_2 \mathcal{L}_2^b + \theta_3 \mathcal{L}_3^b), \quad (15)$$

where θ terms are used to balance the three losses and B is the total number of training samples. For the b -th training sample, \mathcal{L}_1^b , \mathcal{L}_2^b , and \mathcal{L}_3^b are the POI prediction loss, trajectory forecasting loss, and the consistency loss, respectively. The coordinates of each location are normalised so that the scale of three losses are similar.

5 Experiments

In our experiments, we use three widely used LBSNs datasets: Gowalla [6], Foursquare-NYC [42] (FS-NYC), and Foursquare-Tokyo [42] (FS-TKY) (more details of these datasets are contained in Section 7.1 of the *Appendix*). These datasets are publicly available and no personally identifiable information is included. Considering the social connections for FS-NYC and FS-TKY are not given, the method described in Section 4.2 (with $\tau = 0.5$) is used to explore the neighbours of each user. In

Table 1: Performance results (mean \pm std) of different methods on the three datasets. In each row, the best performing results are shown in bold and the second best are given in underline.

	Acc	FMFMGM	LGLMF	RNN	DeepMove	Flashback	STAN	MobTCast
Gowalla	Top-1	0.0394(0.0035)	0.0605(0.0019)	0.1334(0.0021)	0.1636(0.0019)	0.1809(0.0023)	0.1729(0.0015)	0.2051(0.0022)
	Top-5	0.1218(0.0050)	0.1842(0.0049)	0.3040(0.0017)	0.3704(0.0021)	0.3918(0.0018)	0.3875(0.0033)	0.4364(0.0015)
	Top-10	0.1930(0.0058)	0.2793(0.0062)	0.3717(0.0025)	0.4536(0.0022)	0.4710(0.0021)	0.4816(0.0038)	0.5236(0.0022)
	Top-20	0.2976(0.0029)	0.3912(0.0050)	0.4315(0.0026)	0.5196(0.0031)	0.5372(0.0014)	0.5534(0.0028)	0.5956(0.0020)
FS-NYC	Top-1	0.1201(0.0011)	0.0591(0.0038)	0.1960(0.0025)	0.2517(0.0021)	0.2602(0.0028)	0.2755(0.0036)	0.2804(0.0024)
	Top-5	0.3103(0.0014)	0.2122(0.0069)	0.5258(0.0063)	0.5929(0.0032)	0.5992(0.0028)	0.6089(0.0033)	0.6591(0.0031)
	Top-10	0.4054(0.0023)	0.3248(0.0089)	0.6535(0.0102)	0.7013(0.0041)	0.7192(0.0054)	0.7427(0.0037)	0.7816(0.0047)
	Top-20	0.4967(0.0009)	0.4520(0.0113)	0.7464(0.0058)	0.7763(0.0045)	0.8079(0.0038)	0.8398(0.0033)	0.8561(0.0041)
FS-TKY	Top-1	0.0234(0.0061)	0.0334(0.0064)	0.1775(0.0017)	0.1927(0.0027)	0.2303(0.0020)	0.2238(0.0035)	0.2550(0.0048)
	Top-5	0.0690(0.0128)	0.1271(0.0209)	0.4389(0.0026)	0.5023(0.0022)	0.5331(0.0027)	0.5293(0.0039)	0.5683(0.0055)
	Top-10	0.1408(0.0227)	0.2007(0.0110)	0.5397(0.0047)	0.5909(0.0049)	0.6346(0.0054)	0.6245(0.0058)	0.6726(0.0042)
	Top-20	0.2174(0.0178)	0.3495(0.0147)	0.6211(0.0062)	0.6720(0.0065)	0.7082(0.0051)	0.7134(0.0047)	0.7489(0.0054)

our experiments, all visiting records in the training set are used to build check-in vectors so that the social connection of any two users is fixed. Following [41], the observation length n is set to 20 and we split the check-in sequence of each user into 80% for training and 20% for testing.

The hyperparameters are set based on the performance on the validation set which is 10% of the training set. The hidden dimensions for the Transformer used in the mobility feature extractor and the auxiliary task are both 128. According to Eq. (2) and (3), the sum of the dimensions of the POI, semantic and temporal embeddings equals the hidden dimensions of the Transformer $\mathcal{F}(\cdot)$. Thus, we set the dimensions of these embeddings as 80, 24, and 24. As for the weights of three loss functions in Eq. (15), all three θ s are set to 1. For the auxiliary task, we process the dataset by normalising the coordinates within $[-1, 1]$. The model is trained using an Adam optimiser [18] and implemented using PyTorch on a desktop with an NVIDIA GeForce RTX-2080 Ti GPU.

To evaluate the performance of the proposed method, we compare MobTCast against the following POI prediction approaches: FMFMGM [4], a fused matrix factorisation framework using the Multi-centre Gaussian Model to model the geographical information. LGLMF [30], a logistic matrix factorisation method combined with a local geographical model for leveraging geographical information. RNN, the basic architecture for sequential predictions. In the experiments, we use the GRU variant [7] as the baseline. DeepMove [9], a popular RNN-based POI prediction model that incorporates an attention mechanism for modelling the POI visiting history. Flashback [41] and STAN [28], two recent state-of-the-art deep learning-based models for next POI prediction. Similar to [9], we use top- k accuracy ($k = 1, 5, 10, 20$) to evaluate the POI prediction performance. The predicted probabilities of all POIs ($\Pr(\hat{p}_{t+1}^i)$ yield from the main task) are ranked from large to small. We then check whether the actual visited POI (p_{t+1}^i) appears in the top- k predicted POIs.

5.1 Prediction Performance

The results of MobTCast and the baseline methods are given in Table 1. The best performing method on each dataset is given in bold and the second best in underline. For each model, we ran the experiments 5 times and report the average accuracy as well as the standard deviation. In general, deep learning-based methods outperform matrix factorisation-based methods (FMFMGM and LGLMF) by a relatively large margin. The baseline RNN has the worst performance among all deep learning-based methods as no attention mechanism or any context is taken into account. Compared to DeepMove, the weighting function proposed in Flashback is based on temporal and geographical distances, which results in better prediction performance. Overall, with more contexts and the auxiliary task, MobTCast achieves the best performance in comparison to other methods across all datasets.

The original social links of users may be not available in the general case, due to e.g., privacy concerns. The experiments on the FS-NYC and FS-TKY datasets, where social links are not provided, demonstrate that MobTCast is able to handle these datasets by applying a visiting pattern-based process (described in Section 4.2) to discover the ‘‘social’’ context for POI prediction. Such discovered social context can provide useful information for prediction. This also shows the generalisation of MobTCast on different datasets. The average improvement of MobTCast (across all three datasets and all four accuracy metrics) is 7.22%. This improvement is computed as $(acc_1 - acc_2)/acc_2 \times 100\%$, where acc_1 and acc_2 are the accuracy of MobTCast and the second best performing method (either

Table 2: The prediction results of the ablation studies on all three datasets, without (w/o) the specifically mentioned components.

	Gowalla				FS-NYC				FS-TKY			
	TOP-1	Top-5	Top-10	Top-20	TOP-1	Top-5	Top-10	Top-20	TOP-1	Top-5	Top-10	Top-20
V0 (w/o all contexts)	0.1432	0.3374	0.4129	0.4753	0.2219	0.5628	0.6921	0.7723	0.1793	0.4898	0.5882	0.6612
V1 (w/o geographical, w/o social)	0.1691	0.3747	0.4528	0.5192	0.2466	0.6062	0.7338	0.8045	0.2018	0.4966	0.5984	0.6739
V2 (w/o social, w/o \mathcal{L}_2 , w/o \mathcal{L}_3)	0.1896	0.4210	0.5058	0.5766	0.2504	0.6133	0.7417	0.8269	0.2367	0.5459	0.6504	0.7271
V3 (w/o social, w/o \mathcal{L}_3)	0.1925	0.4231	0.5097	0.5796	0.2622	0.6151	0.7476	0.8328	0.2395	0.5463	0.6537	0.7304
V4 (w/o social, w/o \mathcal{L}_2)	0.1934	0.4242	0.5098	0.5813	0.2635	0.6293	0.7606	0.8363	0.2407	0.5483	0.6535	0.7299
V5 (w/o social)	0.1987	0.4332	0.5203	0.5948	0.2727	0.6455	0.7649	0.8457	0.2469	0.5571	0.6641	0.7406
MobTCast	0.2051	0.4364	0.5236	0.5956	0.2804	0.6591	0.7816	0.8561	0.2550	0.5683	0.6726	0.7489

Flashback or STAN depending on the metrics and datasets). These results illustrate the superior prediction performance of the proposed method.

5.2 Ablation study

To investigate the effectiveness of each module in our proposed method, we consider 6 different variants in total (detailed configurations of these variants are given in Section 7.3). The first two variants are: (i) **V0**: None of the three contexts is incorporated in this variant. It can be seen as a mobility feature extractor without using semantic information as input. (ii) **V1**: This variant includes the semantic context only. It predicts the next POI based on the semantic-aware mobility features. Furthermore, given that incorporating the geographical context through the auxiliary task introduces two more loss functions (i.e., trajectory forecasting loss and consistency loss), we also explore the contribution of each loss function through the following 4 variants: (iii) **V2**: This variant only uses the basic POI prediction loss from the main task. (iv) **V3**: The loss function for this variant is a combination of the POI prediction loss and the trajectory forecasting loss from the auxiliary task. (v) **V4**: For this variant, it employs both the POI prediction loss and the proposed consistency loss. (vi) **V5**: All three loss functions are combined in this variant. This loss function is equivalent to the loss function used in MobTCast. For V2 - V4, both semantic and geographical context are enabled. However, the social context extractor used in MobTCast to model the social context is replaced with the basic semantic-aware feature extractor, which means the social context is excluded.

The results (average of 5 runnings) of these variants on the three datasets are given in Table 2. In general, comparing the results from MobTCast against all six variants, it can be noticed that MobTCast outperforms all the variants on all three datasets. V0 yields the worst performance, which is as expected as it is a basic prediction model based on the visiting history without considering any contextual information. When the semantic context is incorporated in V1, compared to V0, we observe that there is a performance gain on all three datasets. With the help of the auxiliary task, variants V2 - V5 have better performances than V0 and V1. More precisely, among these four variants, the performance of V2 is worse than that of the other variants as only the POI prediction loss from the main task is applied and there are no extra constraints for the auxiliary task in the training process. On the contrary, V5 achieves the top performance, where all three loss functions are combined. When only two loss functions are used, V4 outperforms V3 by a relatively small margin. These comparison results confirm the importance of combining both the trajectory forecasting loss and consistency loss when the auxiliary task is introduced. Especially for the consistency loss, it can work as a connection between the two tasks and further improve the POI prediction performance. The results of the above ablation studies show the effectiveness of each module and justify the need for all loss functions included in MobTCast.

6 Conclusion

In this paper, we have proposed MobTCast, a novel deep learning-based architecture to tackle the next POI prediction task. It contains a Transformer-based semantic-aware mobility feature extractor, and a social context extractor to consider the mobility features of the user’s neighbours to take into account the social influence. Furthermore, it includes an auxiliary task, which is a trajectory forecasting task, to incorporate the geographical context. Through extensive experiments, the results illustrate that MobTCast outperforms other state-of-the-art prediction methods and demonstrate the effectiveness of incorporating each type of context in MobTCast. In addition, the main task and the auxiliary task are connected via a consistency loss function. The ablation study results show that introducing the consistency loss function can further improve the performance. A limitation of our approach lies in

that MobTCast depends on contextual information, such as semantic categories. If semantic contexts of places (or social connections) are changed over time, the performance of a trained model might be not optimal. Also, given that the social context extractor takes every neighbour into consideration, the efficiency of our MobTCast would drop if there are too many neighbours. We plan to address these two limitations in future work.

Acknowledgments and Disclosure of Funding

This research is supported by Australian Research Council (ARC) Discovery Project *DP190101485*.

References

- [1] Alexandre Alahi, Kratarth Goel, Vignesh Ramanathan, Alexandre Robicquet, Li Fei-Fei, and Silvio Savarese. Social lstm: Human trajectory prediction in crowded spaces. In *Proceedings of the IEEE conference on computer vision and pattern recognition*, pages 961–971, 2016.
- [2] Michael Backes, Mathias Humbert, Jun Pang, and Yang Zhang. walk2friends: Inferring social links from mobility profiles. In *Proceedings of the 2017 ACM SIGSAC Conference on Computer and Communications Security*, pages 1943–1957, 2017.
- [3] Yile Chen, Cheng Long, Gao Cong, and Chenliang Li. Context-aware deep model for joint mobility and time prediction. In *Proceedings of the 13th International Conference on Web Search and Data Mining*, pages 106–114, 2020.
- [4] Chen Cheng, Haiqin Yang, Irwin King, and Michael Lyu. Fused matrix factorization with geographical and social influence in location-based social networks. In *Proceedings of the AAAI conference on artificial intelligence*, volume 26, 2012.
- [5] Sumanth Chennupati, Ganesh Sistu, Senthil Yogamani, and Samir Rawashdeh. Auxnet: Auxiliary tasks enhanced semantic segmentation for automated driving. *arXiv preprint arXiv:1901.05808*, 2019.
- [6] Eunjoon Cho, Seth A Myers, and Jure Leskovec. Friendship and mobility: user movement in location-based social networks. In *Proceedings of the 17th ACM SIGKDD international conference on Knowledge discovery and data mining*, pages 1082–1090, 2011.
- [7] Junyoung Chung, Caglar Gulcehre, KyungHyun Cho, and Yoshua Bengio. Empirical Evaluation of Gated Recurrent Neural Networks on Sequence Modeling. *arXiv:1412.3555*, 2014.
- [8] Jacob Devlin, Ming-Wei Chang, Kenton Lee, and Kristina Toutanova. Bert: Pre-training of deep bidirectional transformers for language understanding. In *Proceedings of the 2019 Conference of the North American Chapter of the Association for Computational Linguistics: Human Language Technologies, Volume 1 (Long and Short Papers)*, pages 4171–4186, 2019.
- [9] Jie Feng, Yong Li, Chao Zhang, Funing Sun, Fanchao Meng, Ang Guo, and Depeng Jin. Deepmove: Predicting human mobility with attentional recurrent networks. In *Proceedings of the 2018 world wide web conference*, pages 1459–1468, 2018.
- [10] Qiang Gao, Goce Trajcevski, Fan Zhou, Kunpeng Zhang, Ting Zhong, and Fengli Zhang. Trajectory-based social circle inference. In *Proceedings of the 26th ACM SIGSPATIAL International Conference on Advances in Geographic Information Systems*, pages 369–378, 2018.
- [11] Qiang Gao, Fan Zhou, Goce Trajcevski, Kunpeng Zhang, Ting Zhong, and Fengli Zhang. Predicting human mobility via variational attention. In *The World Wide Web Conference*, pages 2750–2756, 2019.
- [12] Rohit Girdhar, Joao Carreira, Carl Doersch, and Andrew Zisserman. Video action transformer network. In *Proceedings of the IEEE Conference on Computer Vision and Pattern Recognition*, pages 244–253, 2019.
- [13] Qing Guo, Zhu Sun, Jie Zhang, and Yin-Leng Theng. An attentional recurrent neural network for personalized next location recommendation. In *Proceedings of the AAAI Conference on Artificial Intelligence*, volume 34, pages 83–90, 2020.

- [14] Qianyue Hao, Lin Chen, Fengli Xu, and Yong Li. Understanding the urban pandemic spreading of covid-19 with real world mobility data. In *Proceedings of the 26th ACM SIGKDD International Conference on Knowledge Discovery & Data Mining*, pages 3485–3492, 2020.
- [15] Sepp Hochreiter and Jürgen Schmidhuber. Long short-term memory. *Neural computation*, 9(8):1735–1780, 1997.
- [16] Hsun-Ping Hsieh and Cheng-Te Li. Inferring online social ties from offline geographical activities. *ACM Transactions on Intelligent Systems and Technology (TIST)*, 10(2):1–21, 2019.
- [17] Jizhou Huang, Haifeng Wang, Miao Fan, An Zhuo, Yibo Sun, and Ying Li. Understanding the impact of the covid-19 pandemic on transportation-related behaviors with human mobility data. In *Proceedings of the 26th ACM SIGKDD International Conference on Knowledge Discovery & Data Mining*, pages 3443–3450, 2020.
- [18] Diederik P Kingma and Jimmy Ba. Adam: A method for stochastic optimization. *arXiv preprint arXiv:1412.6980*, 2014.
- [19] Vineet Kosaraju, Amir Sadeghian, Roberto Martín-Martín, Ian Reid, Hamid Rezaatoughi, and Silvio Savarese. Social-bigat: Multimodal trajectory forecasting using bicycle-gan and graph attention networks. In *Advances in Neural Information Processing Systems*, volume 32, 2019.
- [20] Jiachen Li, Fan Yang, Masayoshi Tomizuka, and Chiho Choi. Evolvegraph: Multi-agent trajectory prediction with dynamic relational reasoning. In *Advances in Neural Information Processing Systems*, volume 33, 2020.
- [21] Xiaolong Li, Gang Pan, Zhaohui Wu, Guande Qi, Shijian Li, Daqing Zhang, Wangsheng Zhang, and Zonghui Wang. Prediction of urban human mobility using large-scale taxi traces and its applications. *Frontiers of Computer Science*, 6(1):111–121, 2012.
- [22] Xutao Li, Gao Cong, Xiao-Li Li, Tuan-Anh Nguyen Pham, and Shonali Krishnaswamy. Rank-geofm: A ranking based geographical factorization method for point of interest recommendation. In *Proceedings of the 38th international ACM SIGIR conference on research and development in information retrieval*, pages 433–442, 2015.
- [23] Defu Lian, Cong Zhao, Xing Xie, Guangzhong Sun, Enhong Chen, and Yong Rui. Geomf: joint geographical modeling and matrix factorization for point-of-interest recommendation. In *Proceedings of the 20th ACM SIGKDD international conference on Knowledge discovery and data mining*, pages 831–840, 2014.
- [24] Dongliang Liao, Weiqing Liu, Yuan Zhong, Jing Li, and Guowei Wang. Predicting activity and location with multi-task context aware recurrent neural network. In *Proceedings of the 27th International Joint Conference on Artificial Intelligence*, pages 3435–3441, 2018.
- [25] Lukas Liebel and Marco Körner. Auxiliary tasks in multi-task learning. *arXiv preprint arXiv:1805.06334*, 2018.
- [26] Qiang Liu, Shu Wu, Liang Wang, and Tieniu Tan. Predicting the next location: A recurrent model with spatial and temporal contexts. In *Thirtieth AAAI conference on artificial intelligence*, 2016.
- [27] Kaiyue Lu, Nick Barnes, Saeed Anwar, and Liang Zheng. From depth what can you see? depth completion via auxiliary image reconstruction. In *IEEE/CVF Conference on Computer Vision and Pattern Recognition (CVPR)*, June 2020.
- [28] Yingtao Luo, Qiang Liu, and Zhaocheng Liu. Stan: Spatio-temporal attention network for next location recommendation. In *The World Wide Web Conference*, 2021.
- [29] Congcong Miao, Ziyang Luo, Fengzhu Zeng, and Jilong Wang. Predicting human mobility via attentive convolutional network. In *Proceedings of the 13th International Conference on Web Search and Data Mining*, pages 438–446, 2020.

- [30] Hossein A Rahmani, Mohammad Aliannejadi, Sajad Ahmadian, Mitra Baratchi, Mohsen Afsharchi, and Fabio Crestani. Lglmf: local geographical based logistic matrix factorization model for poi recommendation. In *Asia Information Retrieval Symposium*, pages 66–78. Springer, 2019.
- [31] Punit Rathore, Dheeraj Kumar, Sutharshan Rajasegarar, Marimuthu Palaniswami, and James C Bezdek. A scalable framework for trajectory prediction. *IEEE Transactions on Intelligent Transportation Systems*, 20(10):3860–3874, 2019.
- [32] Amir Sadeghian, Vineet Kosaraju, Ali Sadeghian, Noriaki Hirose, Hamid Rezatofighi, and Silvio Savarese. Sophie: An attentive gan for predicting paths compliant to social and physical constraints. In *Proceedings of the IEEE/CVF Conference on Computer Vision and Pattern Recognition*, pages 1349–1358, 2019.
- [33] Ke Sun, Tiejun Qian, Tong Chen, Yile Liang, Quoc Viet Hung Nguyen, and Hongzhi Yin. Where to go next: Modeling long-and short-term user preferences for point-of-interest recommendation. In *Proceedings of the AAAI Conference on Artificial Intelligence*, volume 34, pages 214–221, 2020.
- [34] Abhinav Valada, Noha Radwan, and Wolfram Burgard. Deep auxiliary learning for visual localization and odometry. In *2018 IEEE international conference on robotics and automation (ICRA)*, pages 6939–6946. IEEE, 2018.
- [35] Ashish Vaswani, Noam Shazeer, Niki Parmar, Jakob Uszkoreit, Llion Jones, Aidan N Gomez, Łukasz Kaiser, and Illia Polosukhin. Attention is all you need. In *Advances in neural information processing systems*, pages 5998–6008, 2017.
- [36] Xianjing Wang, Flora D Salim, Yongli Ren, and Piotr Koniusz. Relation embedding for personalised translation-based poi recommendation. In *Pacific-Asia Conference on Knowledge Discovery and Data Mining*, pages 53–64. Springer, 2020.
- [37] Yongqiang Wang, Abdelrahman Mohamed, Due Le, Chunxi Liu, Alex Xiao, Jay Mahadeokar, Hongzhao Huang, Andros Tjandra, Xiaohui Zhang, Frank Zhang, et al. Transformer-based acoustic modeling for hybrid speech recognition. In *IEEE ICASSP*, pages 6874–6878. IEEE, 2020.
- [38] Zhumei Wang, Xing Su, and Zhiming Ding. Long-term traffic prediction based on lstm encoder-decoder architecture. *IEEE Transactions on Intelligent Transportation Systems*, 2020.
- [39] Hao Xue, Du Q Huynh, and Mark Reynolds. Poppl: Pedestrian trajectory prediction by lstm with automatic route class clustering. *IEEE transactions on neural networks and learning systems*, 2020.
- [40] Hao Xue and Flora D Salim. Termcast: Temporal relation modeling for effective urban flow forecasting. In *Pacific-Asia Conference on Knowledge Discovery and Data Mining*, 2021.
- [41] Dingqi Yang, Benjamin Fankhauser, Paolo Rosso, and Philippe Cudre-Mauroux. Location prediction over sparse user mobility traces using rnns: Flashback in hidden states! In *Proceedings of the Twenty-Ninth International Joint Conference on Artificial Intelligence, IJCAI-20*, pages 2184–2190, 2020.
- [42] Dingqi Yang, Daqing Zhang, Vincent W Zheng, and Zhiyong Yu. Modeling user activity preference by leveraging user spatial temporal characteristics in lbsns. *IEEE Transactions on Systems, Man, and Cybernetics: Systems*, 45(1):129–142, 2014.
- [43] Di Yao, Chao Zhang, Jianhui Huang, and Jingping Bi. Serm: A recurrent model for next location prediction in semantic trajectories. In *Proceedings of the 2017 ACM on Conference on Information and Knowledge Management*, pages 2411–2414, 2017.
- [44] Jia-Dong Zhang and Chi-Yin Chow. Geosoca: Exploiting geographical, social and categorical correlations for point-of-interest recommendations. In *Proc. of the 38th international ACM SIGIR conference on research and development in information retrieval*, pages 443–452, 2015.
- [45] Muming Zhao, Jian Zhang, Chongyang Zhang, and Wenjun Zhang. Leveraging heterogeneous auxiliary tasks to assist crowd counting. In *Proceedings of the IEEE Conference on Computer Vision and Pattern Recognition*, pages 12736–12745, 2019.

7 Appendix

7.1 Details of Datasets

The details of datasets used in this work are summarised in Table 3. For each dataset, to acquire the user’s check-in sequence, the check-in records of each user are sorted chronologically based on the timestamp given in the dataset. For the semantic information, Foursquare dataset [42] includes low-level semantic category labels (such as Japanese restaurant and Italian restaurant). We then follow the standard Foursquare POI category hierarchy and map each POI to one of the following 8 high-level semantic categories: Arts & Entertainment, College & University, Food, Professional & Other Places, Nightlife Spot, Outdoors & Recreation, Shop & Service, Travel & Transport and Residence. As listed in the table, the semantic category information is not directly given for the Gowalla dataset [6]. ArcGIS is used to decode the semantic information based on the geographical coordinate of each POI. The ArcGIS has the following 11 high-level categories: Arts & Entertainment, Education, Water Features, Travel & Transport, Shops & Service, Residence, Professional & Other places, Parks & Outdoors, Nightlife Spot, Land Features, Food.

In addition, social links are not provided for FS-NYC and FS-TKY. More details about how to discover the social contexts for these datasets are given in Section 4.2. Experiments on such datasets (semantic or social information is not given) could evaluate the generalisation of our method at a certain level.

Table 3: Details of each dataset.

	Gowalla	FS-NYC	FS-TKY
# User	107,092	1,083	2,293
# POI	1,280,969	38,334	61,859
# Check-in	6,442,892	227,428	573,703
Collection Start	2009/02	2012/04	2012/04
Collection End	2010/10	2013/02	2013/02
Semantic Category	No	Yes	Yes
Social Links	Yes	No	No

7.2 Data Driven Analysis

In this part, as a supplement to the discussion in Section 1, we discuss the motivation of incorporating different contexts in POI prediction system from a data-driven perspective.

1. *Semantic Context.* Typically, in LBSNs, each POI belongs to a category with high level semantic meanings such as *Shop* and *Education*. For example, as illustrated in Figure 3(a), there are three visiting peaks (corresponding to breakfast, lunch, and dinner time) for *Food* POIs in each day. As for the *Education*, there is only one morning peak. This shows that POIs with different semantic meanings have different visiting patterns.
2. *Social Context.* Friends and family members often visit a POI together. A user may also check-in a new POI recommended by friends. As shown in Figure 3(b), the average DTW (Dynamic Time Warping, calculated with longitude and latitude coordinates) distance from a user’s trajectory to his/her friends’ trajectories is much smaller than that to other strangers’ trajectories, which reveals that social influence is an important context for predicting POIs.
3. *Geographical Context.* POIs that are close to each other might be visited by the same user due to their proximity. To support and validate the importance of this context, we split each user’s trajectory in a short period (e.g., two consecutive days) into multiple trajectory clips based on the temporal interval between two visits. If the interval is larger than 6 hours, the trajectory will be cut into two clips. We then calculate and compare two statistics: i) the average pair-wise distance between POIs in the same trajectories; and ii) the average pair-wise distance between POIs in different trajectories. As it is shown in Figure 3(c), the distributions of these two distances are different and the distance between POIs in the same trajectories is smaller, which justifies the geographical context.

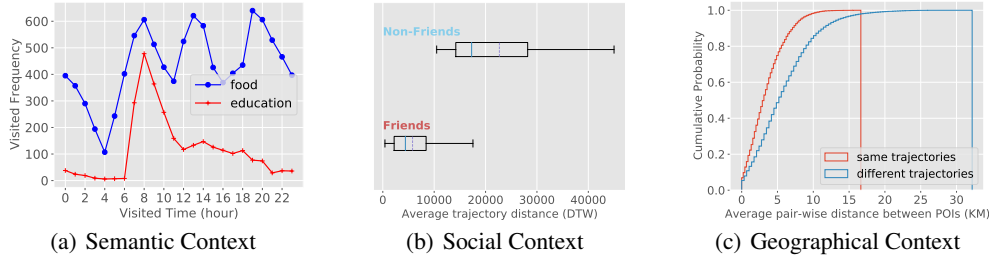


Figure 3: Data-driven motivation of incorporating different contexts. These statistical analysis are based on FS-NYC [42], Gowalla [6], and FS-TKY [42] datasets, respectively.

Table 4: The configuration of each variant.

	Semantic	Geographical	Social	Loss
V0	×	×	×	\mathcal{L}_1
V1	✓	×	×	\mathcal{L}_1
V2	✓	✓	×	\mathcal{L}_1
V3	✓	✓	×	$\mathcal{L}_1 + \mathcal{L}_2$
V4	✓	✓	×	$\mathcal{L}_1 + \mathcal{L}_3$
V5	✓	✓	×	$\mathcal{L}_1 + \mathcal{L}_2 + \mathcal{L}_3$
MobTCast	✓	✓	✓	$\mathcal{L}_1 + \mathcal{L}_2 + \mathcal{L}_3$

7.3 Detailed Configurations of Variants in Ablation Study

All variants compared in Ablation Study (Section 5.2) are summarised in Table 4. In the table, a ✓ indicates that the corresponding context is incorporated, whereas a × means that the context is disabled.

7.4 Auxiliary Task for POI Prediction

In this part of the experiments, we investigate whether we can use the auxiliary task solely to achieve a good POI prediction performance. We aim to answer the research question: can we only use the auxiliary task to predict next POI? Since the outputs from the trajectory forecasting auxiliary task are predicted coordinates (Eq. (9)) instead of probabilities of POIs, it cannot be directly used for predicting the next POI. A tweak is required to get predicted POI from the predicted location. By calculating the Euclidean distances between the predicted location and the locations of all $|P|$ POIs, a $\mathbb{R}^{|P|}$ vector is obtained. The index of the minimum value in this vector is then considered as the predicted POI.

We design two baselines with the tweak operation:

- Aux-RNN: This baseline is an RNN based trajectory forecasting auxiliary task. To be more specific, the forecasting function $\mathcal{F}_g(\cdot)$ in Eq. (6) is a GRU.
- Aux-Tra: This baseline is the same auxiliary task (Transformer based) used in MobTCast (details are given in Section 4.3).

For both Aux-RNN and Aux-Transformer, the user embedding is also applied.

Table 5 lists the POI prediction performance of Aux-RNN and Aux-Transformer on three datasets. For the convenience of comparison, the performance of the proposed MobTCast is also listed in the last row of the table. As shown in the table, it is very clear that both Aux-RNN and Aux-Transformer have poor performance on all datasets, which reveals that these auxiliary tasks and the tweak operation cannot fully model the complex check-in behaviour of each user. More specifically, Aux-Transformer is slightly better than Aux-RNN. Comparing their performances across different datasets, it can be seen that they perform better if the total number of POIs is smaller. This correlation is as expected. Overall, these results indicate that only using the auxiliary task cannot yield good POI predictions.

Table 5: The results of Aux-RNN and Aux-Transformer, where only the auxiliary task is used for POI prediction.

	Gowalla				FS-NYC				FS-TKY			
	TOP-1	Top-5	Top-10	Top-20	TOP-1	Top-5	Top-10	Top-20	TOP-1	Top-5	Top-10	Top-20
Aux-RNN	0.00003	0.0002	0.0003	0.0007	0.0011	0.0023	0.0045	0.0092	0.0004	0.0006	0.0014	0.0046
Aux-Tra	0.00003	0.0002	0.0004	0.0008	0.0017	0.0027	0.0051	0.0106	0.0004	0.0007	0.0019	0.0049
MobTCast	0.2051	0.4364	0.5236	0.5956	0.2804	0.6591	0.7816	0.8561	0.2550	0.5683	0.6726	0.7489

7.5 Computational Cost

In this section, we explore the computation cost of our MobTCast. In Table 6, the inference time (running one training/testing instance) of each deep learning-based model is listed. All these recorded times are executed on the same GPU. Among these methods, the basic RNN (the first row) is the fastest as no other context or attention mechanism is included. Compared to RNN, DeepMove is slightly slower due to the introduced attention calculation in the input history trajectory. Because the attention in Flashback depends on the calculation of temporal and geographical distances (using geographical coordinates), Flashback takes longer for running. As STAN incorporates a bi-layer attention architecture (one attention layer for considering spatio-temporal correlation within user trajectory and one attention layer for recalling the most plausible candidates from all POIs), the inference time of STAN is the largest in the table.

As for our MobTCast_V0, it requires more time than RNN and DeepMove (but less than Flashback) for running. This is because that the Transformer structure which adopts the multi-head attention mechanism is used in MobTCast as the backbone. If we compare V1 against V0, it can be seen that incorporating the semantic context is efficient enough (with a marginal cost increment only). For V2-V5, since the auxiliary trajectory forecasting is introduced, there is a notable increase. However, compared to Flashback where the geographical context is also included, the over-cost of each variant is relatively small. We can also notice that the inference times of these four variants are almost the same. The differences between these variants are about the loss functions (i.e., whether including trajectory forecasting loss and consistency loss), which results in very similar computation costs. Although MobTCast (the last row) needs longer running time than other variants, it takes the social context into accounts. Thus, considering that MobTCast incorporates the computation of social neighbours, the increment of inference time is still acceptable.

Table 6: Comparison of computational cost. Each method is benchmarked on the same NVIDIA GeForce RTX-2080 Ti GPU.

Method	Inference Time (10^{-6} Seconds)
RNN	2.457
DeepMove	3.095
Flashback	29.764
STAN	643.779
MobTCast_V0	16.114
MobTCast_V1	16.550
MobTCast_V2	33.939
MobTCast_V3	33.931
MobTCast_V4	33.913
MobTCast_V5	33.946
MobTCast	127.242

7.6 Weight Setting in Loss Function

As given in Eq. (15), three weight terms are introduced to combine different losses (the POI prediction loss, trajectory forecasting loss, and consistency loss). In this section, we fix $\theta_1 = 1$ and manipulate the rest two weights (θ_2 and θ_3) to fully investigate the influence of these weights. Both θ_2 and θ_3 are set to one of 0.5, 1.0, 2.5, and 5.0, which results in total 16 different combinations. Considering the large amount of the experiments, only the FS-NYC dataset is selected for evaluating. Table 7 reports the POI prediction performance of different combinations on the validation set of FS-NYC dataset. The combination with the best performance for each metric is shown in bold. As it can be seen from

Table 7: Results (on the validation set) of different θ_2 and θ_3 combinations.

Top-1 Accuracy		$\theta_2 = 0.5$	$\theta_2 = 1.0$	$\theta_2 = 2.5$	$\theta_2 = 5.0$
	$\theta_3 = 0.5$	0.2874	0.2874	0.2910	0.2793
	$\theta_3 = 1.0$	0.2883	0.2919	0.2892	0.2739
	$\theta_3 = 2.5$	0.2811	0.2860	0.2829	0.2721
	$\theta_3 = 5.0$	0.2775	0.2865	0.2789	0.2766
Top-5 Accuracy		$\theta_2 = 0.5$	$\theta_2 = 1.0$	$\theta_2 = 2.5$	$\theta_2 = 5.0$
	$\theta_3 = 0.5$	0.6507	0.6529	0.6538	0.6471
	$\theta_3 = 1.0$	0.6430	0.6560	0.6439	0.6484
	$\theta_3 = 2.5$	0.6408	0.6462	0.6372	0.6426
	$\theta_3 = 5.0$	0.6327	0.6453	0.6444	0.6515
Top-10 Accuracy		$\theta_2 = 0.5$	$\theta_2 = 1.0$	$\theta_2 = 2.5$	$\theta_2 = 5.0$
	$\theta_3 = 0.5$	0.8029	0.7881	0.7925	0.7813
	$\theta_3 = 1.0$	0.7867	0.7921	0.7957	0.7966
	$\theta_3 = 2.5$	0.7809	0.7975	0.7777	0.7930
	$\theta_3 = 5.0$	0.7854	0.7952	0.7836	0.7876
Top-20 Accuracy		$\theta_2 = 0.5$	$\theta_2 = 1.0$	$\theta_2 = 2.5$	$\theta_2 = 5.0$
	$\theta_3 = 0.5$	0.8859	0.8877	0.8815	0.8837
	$\theta_3 = 1.0$	0.8788	0.8850	0.8886	0.8859
	$\theta_3 = 2.5$	0.8797	0.8846	0.8841	0.8819
	$\theta_3 = 5.0$	0.8734	0.8909	0.8824	0.8868

the table, the combination of $\theta_2 = 1.0, \theta_3 = 1.0$ achieves top performance in both Top-1 accuracy and Top-5 accuracy, whereas $\theta_2 = 0.5, \theta_3 = 0.5$ and $\theta_2 = 1.0, \theta_3 = 5.0$ is the top performer in Top-10 and Top-20 respectively. Based on these results, in the rest experiments, $\theta_2 = 1.0, \theta_3 = 1.0$ is used as the default setting.

7.7 Different Observation Lengths

In the experiments given in the main paper, the observation length n is set to 20. In this part, we focus on investigating the effect of different observation lengths. Figure 4 shows the performance when the observation length is set to $n = 5, n = 10, n = 20$, and $n = 30$, respectively. As demonstrated from the figure, we can see that the top-5, top-10, and top-20 performance with different observation lengths are quite close. Larger observation length settings ($n = 20$ and $n = 30$) slightly outperform the smaller observation length settings ($n = 5$ and $n = 10$). For the top-1 accuracy, when the observation length is smaller, the performance drops as it is hard to predict when there are only a few visiting records. However, we can also notice that the top-1 performance does not improve when the observation length is too large ($n = 30$). This is because more distant inputs have a relatively smaller contribution (to the next POI) than more up-to-date visiting records.

7.8 Model Training Pseudo-code

In Algorithm 1, the pseudo-code of MobTCast training process. Note that we only use user u_i as an example in the pseudo-code for simplification. In the experiments, all users' data in the training set are included for training and the training instances are processed through mini-batches (batch size 512).

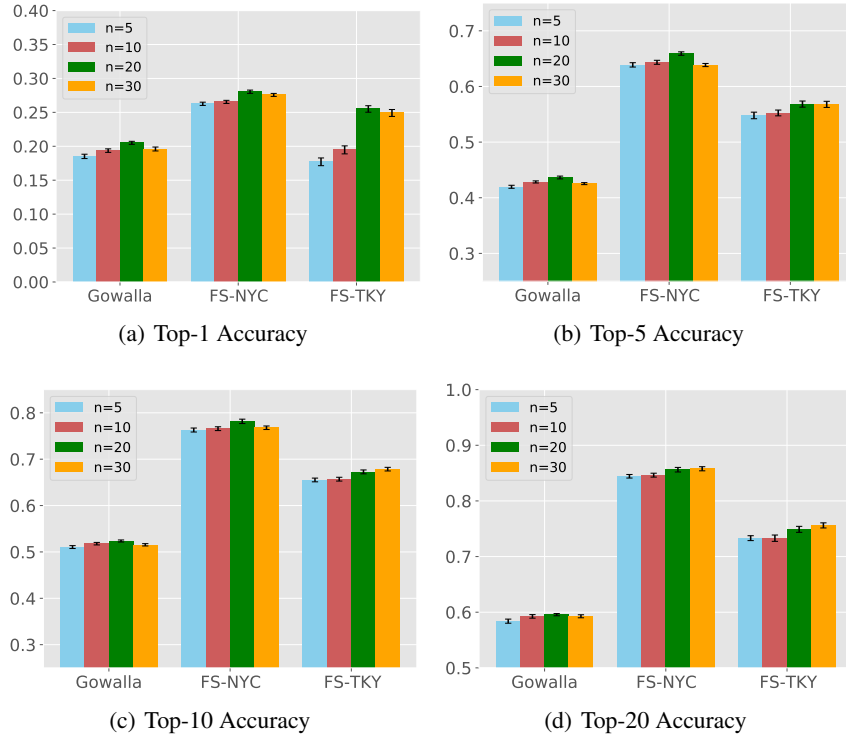


Figure 4: POI prediction performance (on the testing set) with different observation length (n) settings.

Algorithm 1 Pseudo-code of training MobTCast (using one user as an example)

Input: user id: u_i ; observed sequence of user i (visited POI id): P_i ; observed sequence of user i (timestamp id): T_i ; observed sequence of user i (category id): C_i ; observed sequence of user i (geographical coordinate): X_i ; sequences of neighbours: $\{P_j\}, \{T_j\}, \{C_j\}, j \in \mathcal{N}_i$

Output: trained model parameters: γ

- 1: $\gamma \leftarrow$ random initialisation
 - 2: **while** not converge **do**
 - 3: Calculate feature h^i with P_i, T_i, C_i as input by Eqs (1)-(3) \triangleright Semantic-aware mobility feature extraction
 - 4: **for** $j \in \mathcal{N}_i$ **do**
 - 5: Calculate feature h^j with P_j, T_j, C_j as input by Eqs (1)-(3) \triangleright Extract neighbour's mobility feature
 - 6: **end for**
 - 7: Calculate social context vector H^i with h^i and h^j of each neighbour through Eq. (4) \triangleright Model social influence
 - 8: Calculate feature g^i with X_i as input by Eqs (5)-(6) \triangleright Auxiliary branch
 - 9: Embed user id u_i through Eq.(7) \triangleright User embedding
 - 10: Predict the next location (in the geographical coordinate format) by Eqs. (8)-(9) \triangleright Get prediction output of the auxiliary branch
 - 11: Predict the next POI by Eq. (10) \triangleright Get prediction output of the main branch
 - 12: Calculate \mathcal{L}_i with predictions of step 10 and 11 through Eqs (11)-(15) \triangleright Loss calculation
 - 13: Update γ using $\nabla_{\gamma} \mathcal{L}_i$ \triangleright Update model parameters by back propagation
 - 14: **end while**
 - 15: **return** γ
-